Optics Letters

Multipass spectral broadening of 18 mJ pulses compressible from 1.3 ps to 41 fs

Martin Kaumanns,[1,*] Vladimir Pervak,[1] Dmitrii Kormin,[1] Vyacheslav Leshchenko,[1,2] Alexander Kessel,[1,2] Moritz Ueffing,[1] Yu Chen,[2] and Thomas Nubbemeyer[1]

[1]Ludwig-Maximilians-Universität München, Am Coulombwall 1, 85748 Garching, Germany
[2]Max-Planck-Institut für Quantenoptik, Hans-Kopfermann-Str. 1, 85748 Garching, Germany
*Corresponding author: martin.kaumanns@physik.uni-muenchen.de

Received 5 October 2018; revised 2 November 2018; accepted 3 November 2018; posted 5 November 2018 (Doc. ID 347510); published 30 November 2018

Nonlinear compression of laser pulses with tens of millijoule energy in a gas-filled multipass cell is a promising approach to realize a new generation of high average power femtosecond sources. For the first time, to the best of our knowledge, we demonstrate nonlinear broadening of pulses with about 18 mJ of energy at a 5 kHz repetition rate in an argon-filled Herriott cell and show compressibility from 1.3 ps to 41 fs. In addition to the large compression factor, the output beam has an outstanding quality and excellent spectral homogeneity. Furthermore, we discuss prospects to scale the energy to the 100 mJ level in the near future.

https://doi.org/10.1364/OL.43.005877

Nonlinear pulse compression is routinely implemented in fiber-based setups with remarkable results in terms of beam quality, broadening factors, and output energy. Using capillary optical fibers, output energies up to 5 mJ and output pulse durations in the few-cycle regime have been reached for near-infrared laser sources in the kilohertz regime [1]. Using planar hollow waveguide structures [2], more than 10 mJ of output energy have been achieved. Even further energy scaling would yield a unique combination of femtosecond pulse duration with a high peak and average power, leading to a significant increase of photon flux for Thomson X-ray sources [3], which represents the main application for the system presented in this Letter.

In addition to fiber-based approaches, the application of multipass cells for the nonlinear compression of laser pulses recently attracted increasing interest. Multipass cells are capable of preserving a nearly Gaussian mode in the presence of nonlinear effects without a spatial filter or optical fibers [4–6] and are well suited for a large range of pulse energies and repetition rates at high transmission values on the order of 90% [7–12].

In a first experimental realization, 850 fs pulses were compressed in a Herriott cell to 170 fs with M^2 values around 1.3, at 37.5 μJ pulse energy and 10 MHz using fused silica as a nonlinear medium [7]. Subsequent setups based on solid nonlinear materials achieved pulse durations between 18 and 115 fs with microjoule-scale pulse energy and tens of megahertz repetition rate [8–10]. For such setups based on a solid nonlinear medium placed into the propagation path, beam quality preservation is only accomplished for certain cell configurations [6], specifically, configurations close to imaging and strong coupling to higher order modes (e.g., by strong nonlinearities) have to be avoided. Due to these restrictions, a solid-based scheme is typically used for lasers with pulse energies below one millijoule [7,8].

Higher input energies can be realized in gas-filled multipass cells as proposed in Refs. [4] or [5]. In contrast to multipass spectral broadening in solids, the beam continuously interacts with the nonlinear medium in gas-filled cells allowing imaging setups and higher nonlinearities per pass [4,5]. Experimentally, gas-filled multipass cells could reach 1.9 mJ output energy with 37 fs pulse duration [11] and 136 μJ output energy with 33 fs pulse duration [12]. However, while nonlinear broadening in a gas-filled multipass cell is a promising approach for high-energy nonlinear compression, energy scalability beyond 5 mJ as shown by capillary optical fibers [1] has not yet been demonstrated.

In this Letter, we present nonlinear spectral broadening with input energies of 18.6 mJ and a throughput of over 95% at a 5 kHz repetition rate based on a multipass cell inside a chamber filled with 600 mbar of argon and a subsequent compression of attenuated pulses from 1.3 ps to 41 fs. This corresponds to an order of magnitude more input energy and an almost four times higher compression factor than previous nonlinear compression experiments in multipass cells. At the end of this Letter, we will discuss possible optimizations to enable >100 mJ of output energy with a 5 kHz repetition rate and 40 fs pulse duration.

The nonlinear broadening was performed in a Herriott cell [13], as depicted in Fig. 1. The cell consists of two concave rectangular mirrors with a radius of curvature (RoC) of 1.5 m and a size of 300 mm × 130 mm placed in a 4 m long and 0.68 m wide low pressure chamber with a 2 mm thick fused silica window for incoupling. The calculated Gaussian eigenmode for a wavelength of 1030 nm exhibits about a 0.37 mm $1/e^2$ diameter in the focus and a 5.4 mm $1/e^2$ diameter on the mirror surface. Thus, the Herriott cell forms a near

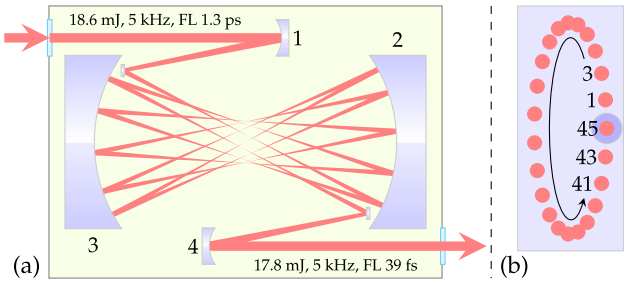

Fig. 1. (a) Scheme of the multipass cell setup (top view) with energy, repetition rate, and Fourier limits (FL) of the input and output pulse. Mirrors 1 and 4 are concave 6 m RoC, and mirrors 2 and 3 are concave 1.5 m RoC. The separation between mirrors 2 and 3 is ∼1.99 times their RoC (≈3 m). (b) Beam pattern on mirror 2. The spots are labeled according to the number of passes through the focus. After 45 passes, the beam is picked by a plane outcoupling mirror.

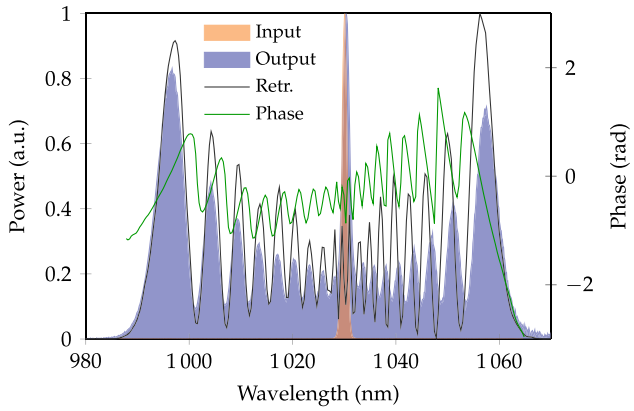

Fig. 2. Measured input (orange) and output (blue) spectra. Additionally depicted are the retrieved spectrum (black) and phase (green) from the SHG-FROG measurement of the compressed pulse.

concentric cavity operated close to its stability edge. The chamber is filled with 600 mbar of argon for the following results (if not mentioned otherwise), but can be used with pressures up to 1 bar. The mirrors were ion-beam-sputtering-coated in house with zero group delay dispersion (GDD) at 1030 nm and $|\mathrm{GDD}| < 50$ fs^2, as well as a reflectivity of >99.9% between 965 and 1100 nm. The laser-induced damage threshold was measured to be about 0.25 J/cm^2 in experimental conditions.

The beam is mode matched to the eigenmode of the Herriott cell by a 6 m RoC concave mirror (mirror 1 in Fig. 1). A 1″ plane mirror placed in front of the large rectangular mirror steers the beam into the Herriott cell. The cell is aligned such that the beam pattern on mirrors 2 and 3 is elliptical. This pattern ensures an efficient usage of mirror space, while still having a large beam separation at the point of incoupling/outcoupling and a preservation of the q-preserving properties of the Herriott cell. After 45 passes (one pass is one transition through a focus), a second plane mirror guides the beam onto a 6 m RoC concave collimation mirror. Thus, the output beam size matches the input beam size.

The Yb:YAG thin-disk amplifier presented in [14], in combination with a modified frontend based on a fiber laser oscillator, is used as a source. The system delivers up to 200 mJ of pulse energy at a 5 kHz repetition rate with 1.3 ps full width at half-maximum (FWHM) pulse duration. Its spectrum is centered at 1030 nm with a bandwidth of 1.1 nm (labeled *Input* in Fig. 2) and its $1/e^2$ diameter is 11 mm. A low order waveplate, in combination with a thin film polarizer, is used to control the input power into the multipass cell. To guarantee reliable operation, the peak fluence on mirrors 2 and 3 was adjusted to 66% of the damage threshold or, equivalently, 0.17 J/cm^2 corresponding to a pulse energy of 18.6 mJ.

The measured output energy of 17.8 mJ yields a transmission of 95.7%, which fits the expected linear losses determined by the number of passes and the reflectivity of the mirrors. Thus, no significant nonlinear losses, e.g., due to ionization, were detected. For further analysis, the output beam is attenuated using a pair of uncoated fused silica wedges and reduced in size by a factor of four using a lens telescope.

The measured output spectrum, as shown in Fig. 2, is a result of self-phase modulation (SPM) with a Fourier limit of 39 fs. Compared to the input Fourier limit of 1.3 ps, this is equivalent to a broadening factor of over 33. SPM causes a time-domain phase modification that has the same shape as the pulse intensity, thereby broadening the spectrum. In this experiment, the textbook equation for SPM (Ref. [15], p. 91),

$$I(\omega) \approx |\mathcal{F}[A(t)\exp(i\varphi|A(t)|^2)]|^2, \quad \textbf{(1)}$$

with the Fourier transform $\mathcal{F}[\cdot]$, the normalized input pulse amplitude $A(t)$, and a total nonlinear phase shift φ, qualitatively reproduces the output spectrum, except for a central peak that is caused by a low-intensity background originating from amplified spontaneous emission as well as post- and pre-pulses. A fit of the measured output spectrum (Fig. 2) to a theoretical spectrum $I(\omega)$ calculated by Eq. (1) reveals an accumulated phase shift of $\varphi \approx 55$ rad. This is in agreement with the expected phase shift [5] of 59 ± 6 rad for 45 dispersion-free passes of the Gaussian eigenmode in 600 mbar of argon (n_2, 1 bar $\approx (10 \pm 1) \times 10^{-24}$ m^2/W [16]). The spatially averaged nonlinear phase shift per pass is $\varphi_{\mathrm{pass}} \approx 1.2$ rad, which is more than three times higher as compared to the systems presented in [7–12] ($\varphi_{\mathrm{pass}} \approx 0.2$–$0.4$ rad), allowing high broadening factors with a comparably small number of passes.

Typically, secondary SPM effects such as optical wave breaking and self-steepening pose limitations for high broadening factors ([15], p. 100 ff). However, the agreement between a spectrum described by Eq. (1) and our measurement confirms that in our experiment processes other than pure SPM have only a minor impact on the output. The main reason for the lack of secondary effects is the weak GDD of about 1150 fs^2 for 45 passes at 1030 nm in argon [17], the negligible GDD of the mirrors, and the picosecond-scale pulse duration. For these parameters, the nonlinear phase shift of ∼55 rad is far below the calculated critical values for wave breaking ($\varphi_{\mathrm{WB}} \approx 589$ rad [18]) and self-steepening ($\varphi_{\mathrm{SS}} \approx 555$ rad [Ref. [15], p. 117]). The insignificant influence of dispersion [19] and self-steepening on the output bandwidth enable the observed high broadening factor.

The spatio-spectral homogeneity of the beam was measured using an imaging spectrometer (*Acton Research Corporation*) (Fig. 3). The spatial resolution was 36 μm, and the spectral resolution was 0.24 nm. A figure of merit called homogeneity is defined as $V = [\int A(\lambda)A_0(\lambda)\mathrm{d}\lambda]^2/[\int A(\lambda)^2\mathrm{d}\lambda \int A_0(\lambda)^2\mathrm{d}\lambda]$

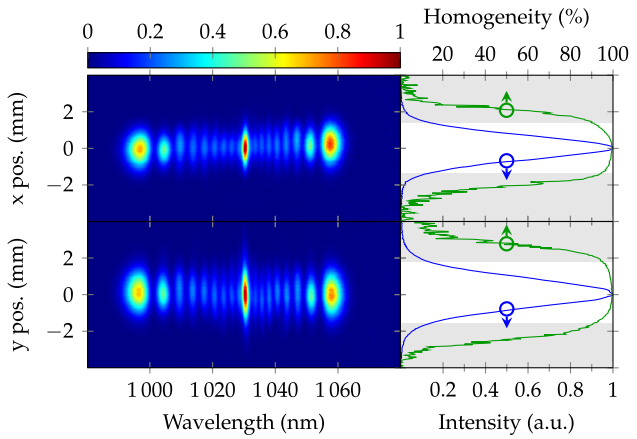

Fig. 3. Spatial wavelength distribution for the x and y axis of the output beam. The blue curve on the right shows the normalized sum along the wavelength axis of the image on the left. The white area marks the positions where this normalized sum is bigger than $1/e^2$. The green curve shows the corresponding homogeneity value.

[8] where $A(\lambda)$ is the spectral amplitude, and $A_0(\lambda)$ is the reference amplitude at a maximum intensity of the beam. The output spectrum features high homogeneity values over 90% within the $1/e^2$ diameter for both axes. The intensity-weighted averages of V over the beam are 96.7% for the x-axis and 97.3% for the y-axis.

The excellent spatial quality of the beam is confirmed by an M^2 measurement (Ophir Spiricon M^2-200 s, Fig. 4). The M^2 of the laser source is 1.10 × 1.09 [14]. It slightly increases after propagation through the multipass system in vacuum condition to 1.15 × 1.11. The increase is attributed to the imperfectness of curved optics, in combination with 45 mirror bounces. After filling the chamber with 600 mbar of argon, the M^2 further increases to 1.17 × 1.18. This minor change is attributed to the nonlinear effects that are not compensated for by the multipass setup.

To analyze the compressability, the attenuated pulses with an energy of 20 μJ are guided through a chirped mirror compressor (17 mirrors with a total GDD of –9400 fs^2 and a total reflectivity of 98%) and characterized using a second-harmonic-generation frequency-resolved optical gating (SHG-FROG) setup. The attenuation avoids nonlinear contributions of air and damages of the used chirped mirrors. A compressor suitable for high energies is currently under development.

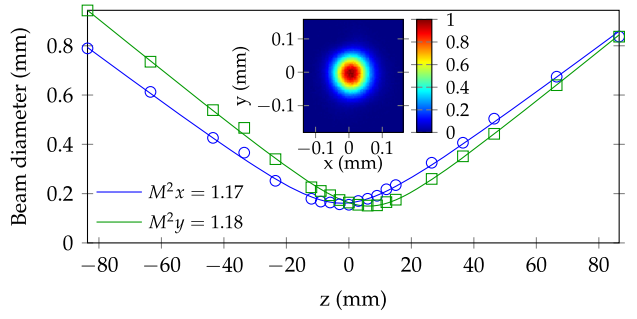

Fig. 4. Beam quality factor (M^2) of the output beam. The inset shows the beam profile in the focus ($z = 0$).

Figure 5(b) shows the SHG-FROG measurement and retrieval with a SHG-FROG error of 1.5% on a 512 × 512 grid. The retrieved spectrum, together with the retrieved phase, is depicted in Fig. 2 and shows excellent agreement with the measured spectrum. The retrieved pulse is depicted in Fig. 5(a). The FWHM pulse duration of 41 fs is close to the Fourier limit of 39 fs, while the peak power of the measured pulse is 62% of the measured Fourier limited power. Perfect compression is hindered by the phase oscillations visible in Fig. 2 that are hardly removable by common compression techniques. The duration and power are in accordance with the simulated values of 41.6 fs and 67%, correspondingly. The simulation is performed by approximating the field amplitude of the broadened pulse by the expression $A_{\text{out}}(t) = A(t)\exp(i\varphi|A(t)|^2)$ [see Eq. (1)] with $\varphi = 55$ rad and $A(t)$ being the input pulse amplitude [see Fig. 5(a)] and removing the GDD component of the phase term.

The output energy is limited by the gas ionization and mirror damage threshold. In our experimental conditions (45 passes in argon), gas ionization at high intensities causes a spontaneous sudden and intense drop of output energy to almost zero. The lowest output energy at which a sudden drop of energy occurred is referred to as breakdown energy. In our configuration, the measured breakdown energy for argon at 600 mbar is about 18.3 mJ (see Fig. 6). The observed relatively strong pressure dependency of $p^{-1/2.5}$ deviates from the expected value of $\sim p^{-1/14}$ for pure multiphoton ionization [20], but can be explained by the decreasing waist size due to the Kerr effect or the onset of cascade ionization [20]. Although the energy in the presented setup is close to the measured

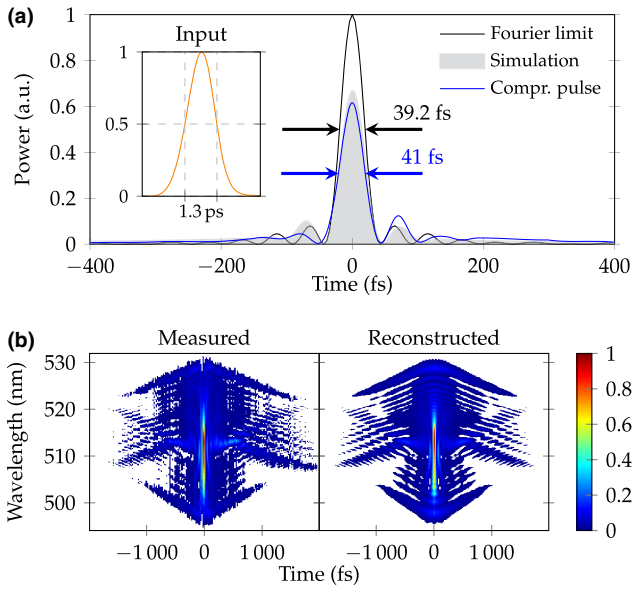

Fig. 5. (a) Fourier-limited pulse calculated from the output spectrum shown in Fig. 2 (black), together with the retrieved compressed pulse (blue) and a simulation of the nonlinear compression (gray). The arrows mark the FWHM durations of the Fourier-limited pulse (black) and the compressed pulse (blue). The measured input pulse and its FWHM duration are shown in the inset. (b) Measured (left) and the retrieved (right) SHG-FROG intensity for the compressed pulse in (a).

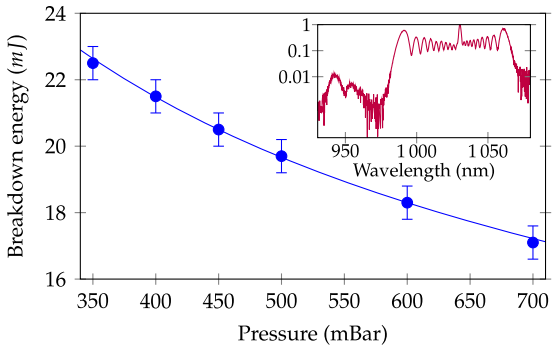

Fig. 6. Argon breakdown energy versus pressure for this setup. A pressure dependency of $\propto p^{-1/2.5}$ is shown as a solid line. The inset depicts the output spectrum near a breakdown for 0.7 bar.

breakdown energy, no breakdown was observed during our measurements (>3 h).

To test the broadening limits of the presented system, the pressure was further increased to 700 mbar. The input energy was reduced to 17 mJ to avoid a gas breakdown. The M^2 value changed slightly to 1.16 × 1.19, indicating good beam quality preservation. Yet, the increase of the pressure results in a distorted spectrum with new wavelengths around 950 nm (see Fig. 6) and degraded compression that occurs most probably due to the limited bandwidth of the used mirrors. Therefore, a more broadband coating might lead to a higher compression factor.

In order to work with higher input energies, larger beam diameters in the focus are required. Due to diffraction this leads to smaller beam diameters on the mirrors and overall results in an energy scaling proportional to the square root of the mirror damage threshold. As an example, increasing the damage threshold from 0.25 to 1 J/cm^2 would allow a two times higher energy. A second possibility to increase the energy throughput is the usage of a different gas. In our experiments, helium had a breakdown value on the order of two–three times higher than argon at the same pressure (similar results were obtained in [21]). Analogous to the scaling with mirror damage threshold, the energy throughput increases with the square root of the breakdown value. Disadvantageous is the 28 times lower nonlinear refractive index of helium compared to argon (0.36×10^{-24} m^2/W for helium [22] and 10×10^{-24} m^2/W for argon [16]) which could be compensated for using a chamber compatible with several bars of pressure. This pressure range exceeds the current capabilities of our setup and will be incorporated in a future implementation of the multipass cell. A third option is to increase the setup length, yielding a linear increase of energy throughput. Combining an improved damage threshold with an 8 m long chamber that is prepared for high pressures should enable energies beyond 100 mJ with a compression from 1.3 ps to about 40 fs.

In conclusion, we demonstrated the scaling of nonlinear broadening in gas-filled multipass cells to 17.8 mJ pulse energy with a repetition rate of 5 kHz. A compression factor of over 31 was achieved with output pulses of 41 fs FWHM duration for an input duration of 1.3 ps. The throughput of the cell was 95.7% with nearly Gaussian output beams showing M^2 values of 1.17 × 1.18. The output beam was spatially homogeneous with intensity-weighted average homogeneities of about 97%. To the best of our knowledge, this is the highest output energy spectrally broadened with preserved beam quality. Even higher energies can be obtained by optimizing the mirror damage threshold, lengthening the setup, and changing the gas from argon to helium. The possible output energy after these changes is >100 mJ with high repetition rates of multiple kilohertz. The energy scalability of multipass cells has the capability to combine femtosecond-scale pulse durations with the high average power of ytterbium amplifiers and, by this means, to provide unprecedented laser properties.

Funding. Munich-Centre for Advanced Photonics (MAP).

Acknowledgment. The authors gratefully acknowledge the support of Prof. Ferenc Krausz. Furthermore, they thank Jonathan Brons and Simon Reiger for their useful remarks and Nicholas Karpowicz for his help in preparing this Letter.

REFERENCES

1. S. Bohman, A. Suda, T. Kanai, S. Yamaguchi, and K. Midorikawa, Opt. Lett. **35**, 1887 (2010).
2. C. L. Arnold, B. Zhou, S. Akturk, S. Chen, A. Couairon, and A. Mysyrowicz, New J. Phys. **12**, 073015 (2010).
3. R. Behling and F. Grüner, Nucl. Instrum. Methods Phys. Res. A **878**, 50 (2018).
4. N. Milosevic, G. Tempea, and T. Brabec, Opt. Lett. **25**, 672 (2000).
5. M. Hanna, X. Délen, L. Lavenu, F. Guichard, Y. Zaouter, F. Druon, and P. Georges, J. Opt. Soc. Am. B **34**, 1340 (2017).
6. P. Russbueldt, J. Weitenberg, A. Vernaleken, T. Sartorius, and J. Schulte, "Method and arrangement for spectral broadening of laser pulses for non-linear pulse compression," U.S. patent 9,847,615 (December 19, 2017).
7. J. Schulte, T. Sartorius, J. Weitenberg, A. Vernaleken, and P. Russbueldt, Opt. Lett. **41**, 4511 (2016).
8. J. Weitenberg, A. Vernaleken, J. Schulte, A. Ozawa, T. Sartorius, V. Pervak, H.-D. Hoffmann, T. Udem, P. Russbüldt, and T. W. Hänsch, Opt. Express **25**, 20502 (2017).
9. J. Weitenberg, T. Saule, J. Schulte, and P. Rußbüldt, IEEE J. Quantum Electron. **53**, 1 (2017).
10. K. Fritsch, M. Poetzlberger, V. Pervak, J. Brons, and O. Pronin, Opt. Lett. **43**, 4643 (2018).
11. M. Ueffing, S. Reiger, M. Kaumanns, V. Pervak, M. Trubetskov, T. Nubbemeyer, and F. Krausz, Opt. Lett. **43**, 2070 (2018).
12. L. Lavenu, M. Natile, F. Guichard, Y. Zaouter, X. Delen, M. Hanna, E. Mottay, and P. Georges, Opt. Lett. **43**, 2252 (2018).
13. D. R. Herriott and H. J. Schulte, Appl. Opt. **4**, 883 (1965).
14. T. Nubbemeyer, M. Kaumanns, M. Ueffing, M. Gorjan, A. Alismail, H. Fattahi, J. Brons, O. Pronin, H. G. Barros, Z. Major, T. Metzger, D. Sutter, and F. Krausz, Opt. Lett. **42**, 1381 (2017).
15. S. Zahedpour, J. K. Wahlstrand, and H. M. Milchberg, Opt. Lett. **40**, 5794 (2015).
16. E. R. Peck and D. J. Fisher, J. Opt. Soc. Am. **54**, 1362 (1964).
17. D. Anderson, M. Desaix, M. Lisak, and M. L. Quiroga-Teixeiro, J. Opt. Soc. Am. B **9**, 1358 (1992).
18. G. Agrawal, *Nonlinear Fiber Optics*, 5th ed. (Academic, 2013).
19. A. Zheltikov, Opt. Express **26**, 17571 (2018).
20. R. K. Avery, J. Phys. D **17**, 1657 (1984).
21. C. L. M. Ireland and C. G. Morgan, J. Phys. D **6**, 720 (1973).
22. J. Bernhardt, P. Simard, W. Liu, H. Xu, F. Théberge, A. Azarm, J. Daigle, and S. Chin, Opt. Commun. **281**, 2248 (2008).